

OPTIMUM PERFORMANCE OF GREEN MACHINING ON THIN WALLED Ti6Al4V USING RSM AND ANN IN TERMS OF CUTTING FORCE AND SURFACE ROUGHNESS

Muhammad Yanis^a, Amrifan Saladin Mohruni^{a*}, Safian Sharif^b, Irsyadi Yani^a

^aMechanical Engineering Department, Sriwijaya University, 30662, Inderalaya, Ogan Ilir, South Sumatera, Indonesia

^bSchool of Mechanical Engineering, Faculty of Engineering, Universiti Teknologi Malaysia, 81310 UTM Johor Bahru, Johor, Malaysia

Article history

Received

25 December 2018

Received in revised form

20 June 2019

Accepted

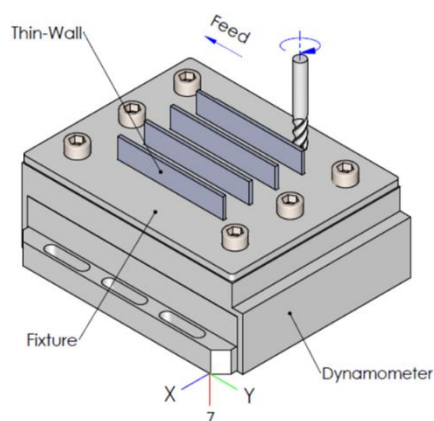
15 July 2019

Published online

24 October 2019

*Corresponding author
mohrunias@unsri.ac.id

Graphical abstract



Abstract

Thin walled titanium alloys are mostly applied in the aerospace industry owing to their favorable characteristic such as high strength-to-weight ratio. Besides vibration, the friction at the cutting zone in milling of thin-walled Ti6Al4V will create inconsistencies in the cutting force and increase the surface roughness. Previous researchers reported the use of vegetable oils in machining metal as an effort towards green machining in reducing the undesirable cutting friction. Machining experiments were conducted under Minimum Quantity Lubrication (MQL) using coconut oil as cutting fluid, which has better oxidative stability than other vegetable oil. Uncoated carbide tools were used in this milling experiment. The influence of cutting speed, feed and depth of cut on cutting force and surface roughness were modeled using response surface methodology (RSM) and artificial neural network (ANN). Experimental machining results indicated that ANN model prediction was more accurate compared to the RSM model. The maximum cutting force and surface roughness values recorded are 14.89 N, and 0.161 μm under machining conditions of 125 m/min cutting speed, 0.04 mm/tooth feed, 0.25 mm radial depth of cut (DOC) and 5 mm axial DOC.

Keywords: Optimization, green machining, thin-walled Ti6Al4V, RSM, ANN, cutting force, surface roughness

Abstrak

Kebanyakan aplikasi aloi titanium berketebalan nipis dalam industri aeroangkasa adalah disebabkan kelebihan ciri seperti nisbah kekuatan-terhadap-berat yang tinggi. Di samping getaran, geseran pada zon pemotongan semasa mengisar aloi titanium berketebalan nipis akan menghasilkan ketakkonsistenan/ketaktekalan daya pemotongan dan meningkatkan kekasaran permukaan. Penyelidik terdahulu melaporkan bahawa penggunaan minyak sayuran di dalam pemesinan logam adalah sebagai usaha menuju pemesinan hijau bagi mengurangkan geseran yang tidak diingini. Ujian pemesinan telah dijalankan menggunakan Kuantiti Pelinciran Minimum (MQL) dengan minyak kelapa sebagai cecair pelincir, yang mempunyai lebih kesetabilan oksidatif berbanding dengan minyak sayuran yang lain. Mataalat karbida tanpa salutan telah digunakan dalam ujian pemesinan. Pengaruh halaju pemotongan, uluran dan kedalaman

pemotongan ke atas daya pemotongan dan kekasaran permukaan telah dimodelkan menggunakan RSM dan ANN. Keputusan ujikaji pemesinan menunjukkan ramalan model ANN memberi ketepatan yang lebih baik berbanding dengan model RSM. Daya pemotongan yang maksimum dan nilai kekasaran permukaan yang direkodkan, masing-masing adalah 14.89 N dan $0.161 \mu\text{m}$ di bawah keadaan pemesinan 125 m/min halaju pemotongan, 0.04 mm/uluran, 0.25 mm kedalaman pemotongang radial dan 5 mm kedalaman pemotongan aksial.

Kata kunci: Pengoptimuman, pemesinan hijau, Ti-6Al4V berketebalan nipis, RSM, ANN, daya pemotongan, kekasaran permukaan

© 2019 Penerbit UTM Press. All rights reserved

1.0 INTRODUCTION

Thin-walled parts are considerably used in many fields of component products such as aerospace, marine, and power industry [1]. Titanium alloys thin-walled in many directions are applied in the aerospace industry owing to their excellent property in the aerospace environment such as light weight, superior resistance to oxidation, lower density, fracture, and fatigue [2], [3]. Ti6Al4V is often used among all titanium alloys because of its high strength, good toughness, and superior resistance to corrosion [2].

During the milling of thin-walled parts, the thin part tends to deform under the action of cutting force [4]. The serrated chips at thin walled caused by elevated cutting zone temperature can significantly promote the formations of built-up edge (BUE) on the tooltip. The presence of BUE will create inconsistent in the cutting force and make surface quality worse [2], [5], [6]. A complex structure of thin-walled and inferior processing technology conduce surface quality challenging to control and give rise to the machining accuracy cannot be guaranteed [4].

The surface roughness mechanism depends on the machining process. The decreased cutting force, which caused the reduced cutting temperature, was generated by the decline of feed rate and cutting speed [7]. Conversely, the decrease in cutting speed improves a surface, not productivity [8]. The combination between restrict the cutting speed and high-efficiency machining should improve the cutting efficiency of machining titanium alloy. Therefore to manage the cutting load is essential to work [2].

Proper comprehensive methods in using cutting fluid may significantly reduce the temperature in machining, and thus, the surface roughness would be better [9]. International Agency for Research on Cancer (IARC) reported that petroleum-based cutting fluids which contain heterocyclic and polyaromatic rings are carcinogenic and could result in occupational skin cancer [8]. It has been reported during the year 1993 that around 16% of industrial diseases in Finland were caused by cutting fluids. These diseases are connected to the skin and musculoskeletal [10].

Many industries start to concern a cleaner production on their machining process [8]. The objectives in the ISO 14000 family is to preserve the environment in balance with socioeconomic [11]. These requirements have led to scientific research toward green machining, such as the use of vegetable oil as cutting fluid [8]. Coconut oil has oxidative stability higher than that of other vegetable oils in machining industries [12]. The performance of coconut oil on turning of AISI 304 showed superior surface roughness than soluble oil and straight cutting oil [8]. A study reported sesame and coconut oil with additives in machining AISI 1040 steel, which coconut oil reduced the cutting force by 20% compared to other considered fluids [6].

The industry is prospecting methods for reducing consumption of cutting fluid during metal cutting operation because of the ecological requirement if using petroleum cutting fluid and economic reason. The high consumption of cutting fluid also results in huge expenses [9]. It is measurable that almost 20-30% of total industrial costs are related to the using of cutting fluid during hard machining. Minimum quantity lubrication (MQL) apply less cutting fluid, which flows rates ranging from 2 to 14 ml/h [10]. The increase in MQL flow rate up to a certain point reduce cutting force. The use of high air pressure in MQL generated the oil droplets which penetrate the cutting zone and decrease cutting energy and friction [5].

Boswell (2017) reviewed many studies about MQL, some of the studies reported about milling of titanium aluminides intermetallic alloy and turning which MQL could lower the surface roughness and cutting force if compared to dry and flood strategy. Muhammed (2016), in his review, recorded that MQL is comparatively superior to dry and flood at higher cutting speed in machining titanium alloy. The study was written by Vishal (2015) also informed that the influence of MQL conduced reduction in cutting force and surface roughness significantly in milling Ti6Al4V. Drilling Ti6Al4V under MQL using palm oil generated the surface roughness seems to be smoother than that for the MQL synthetic ester during increasing in cutting speed 100 m/min. However, the increasing feed rate levels bring out to an increase in the surface roughness [13]. Ti6Al4V would harden during milling under MQL

commercial vegetable oil if cryogenic were applied. Hence the cutting force increased but cutting force decrease if the flow rate of cutting fluid increases [5]. This research intended to investigate the influence of cutting speed, feed rate, and depth of cut on the cutting force and surface roughness in the milling process. The carried out process was milling the thin-walled Ti6Al4V under MQL using uncoated carbide tools. The uncoated WC-Co insert tools are recommended for machining Ti6Al4V [14]. There was research about machining Ti6Al4V by MQL, dry, and flood to analyzed cutting force and surface roughness, which used uncoated carbide insert [11]. Uncoated carbide tools also used in drilling Ti6Al4V under MQL [10]. Gururaj (2017) recorded the using of uncoated carbide tools in the milling of aerospace titanium alloy Ti-6242S under dry cutting condition. Even, uncoated carbide cutting tools used in turning Ti6Al4V under a dry cutting condition at a cutting speed of 150 m/min [15].

The influence of cutting load as variable machining of the milling system is uncertain not only came from the use or not use of cutting fluid, but the system is nonlinear behavior [7]. Other problems are conducting experiments time-consuming and prone to error [16]. Therefore, recently, many investigations have focused on the modeled prediction, such as surface topography to optimization machining [3]. RSM, as the mathematical and statistical approach, applies to optimization variables. The coupling method of response surface used in the optimization of cutting force and surface roughness in machining Ti6Al4V under MQL using vegetable oil [11]. ANN methods recorded has been used in the optimization of surface roughness in machining Ti6Al4V under EDM process [17]. This research applied RSM in predicting and optimization of cutting force and surface roughness. RSM methods compared with an artificial neural network (ANN) to investigate the closeness to experiment data.

2.0 METHODOLOGY

2.1 Tool and Material

The thin wall milling using WC Co uncoated end mill with 10 mm, 4 flute and the helical angle is 47° (produced by HPMT). The workpiece material used in this experiment was Ti6Al4V grade-5. This material is an aerospace grade commercial titanium alloy. These workpieces were prepared by EDM-Wire Cut and dimension thin wall 3 × 20 × 100 mm. Figure 1, as shown workpiece mounted at dynamometer by the specific fixture. Mechanical and chemical properties of the Ti6Al4V is given in Table 1.

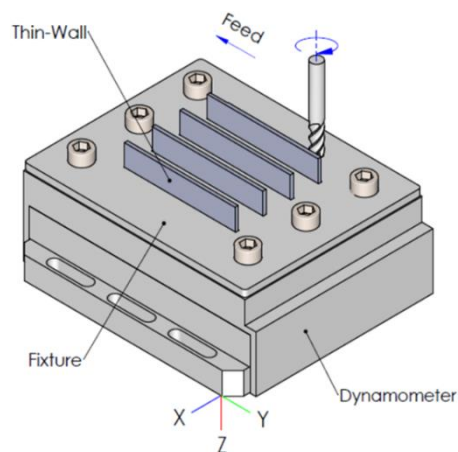


Figure 1 Thin wall fixed on a dynamometer

Table 1 Chemical and mechanic properties of Ti6Al4V

Chemical Composition (wt %)							
Ti	Al	V	C	Fe	N	O	H
Balance	6.39	4.15	0.01	0.21	0.1	0.17	0.001
Mechanical Properties							
Tensile Strength	(MPa)	:					940
Yield Strength 0.2%	(MPa)	:					865
Elongation	(%)	:					15.6
Reduction of Area	(%)	:					38

2.2 Cutting Fluid

The milling experiments used coconut oil as cutting fluids. The cutting fluid was obtained from a local market and locally produced. Cutting fluids as environmentally friendly was operated using the Minimum Quantity Lubrication (MQL) system with a capacity of 40 ml/hour. The specification of the cutting fluid is shown in Table 2.

Table 2 Specifications of coconut oils

Parameters, Unit	Value
1. Density @ 15°C, kg/m ³	925.8
2. Flash Point, °C	286.0
3. Kinematic Viscosity @100°C, cSt	6.069

2.3 Experimental Setup

All experiments were performed on a MAHO DMC 835 V CNC 3 axis VMC with Fanuc Controller model, maximum spindle 14000 rpm and power 15 kW. The Kistler dynamometer (model 9265B) was used for measuring the resultant force (F). During the experiment test, the radial force (x-direction), tangential force (y-direction) and axial force (z-direction) were recorded simultaneously. The analyzed cutting force (F_c) was the tangential force according to the reference system of metal cutting. The resulted surface roughness (R_a) was measured using a surface roughness tester Accretech Handysurf

type E-35 A/E. The parameters of measurement are 0.8 mm and 4.0 mm for cut off (CO) and length of cut (LoC), respectively.

2.4 Design of Experiments (DOE)

In this study, the Rotatable Central Composite Design (RCCD) was used. As the independent variables, the cutting speed (V_c), feed rate (f_z), radial DOC (a_r), and axial DOC (a_x) were applied. Whereas, the R_a and the F_c are chosen as dependent variables. The RCCD used consists of the 2^k factorial design, which is augmented with a star point for each axial coordinate. The distance (α) between the star and center points is equal to 2 [18]. The coded values of every level obtained from Equation 1.

$$x = \frac{\ln x_n - \ln x_{n0}}{\ln x_{n1} - \ln x_{n0}} \tag{1}$$

where x_n is the value of any factor corresponding to its natural value, moreover, x_{n1} is the value of factor at the level +1, while the x_{n0} is the natural value of the factor corresponding to the base or level zero. The values in each level were listed in Table 3.

Table 3 The level and coding of independent variables

Independent Variable	Levels				
	-2	-1	0	+1	+2
V_c (m/min)	64.00	80	100	125	156.25
f_z (mm/tooth)	0.025	0.04	0.063	0.1	0.158
a_r (mm)	0.200	0.25	0.32	0.4	0.51
a_x (mm)	3.536	5	7.07	10	14.17

Data analysis were carried out using RSM and ANN. Many researchers reported that both methods are capable of finding the optimum result [19], [20], [21].

2.5 Response Surface Methodology (RSM)

RSM is a statistical procedure, and mathematical modeling used for developing, improving, and optimizing of process. In this experiment, a prediction model for dependent variables can be expressed in Equation 2, and Equation 3.

$$F_c = C_1 V_c^k f_z^l a_r^m a_x^n \epsilon_1 \tag{2}$$

$$R_a = C_2 V_c^o f_z^p a_r^q a_x^r \epsilon_2 \tag{3}$$

where R_a is the surface roughness, F_c is the cutting force, V_c is the cutting speed, f_z is the feed rate, a_r and a_x are the radials and axial depth of cut, ϵ is the experimental errors, and C, k, l, m, n are the constant of R_a and F_c . The constants of Equation 2 and Equation 3, were determined by conversion a linear form with a

logarithmic transformation, as shown in Equation 4 and Equation 5:

$$\ln F_c = \ln C_1 + k \ln V_c + l \ln f_z + m \ln a_r + n \ln a_x + \ln \epsilon_1 \tag{4}$$

$$\ln R_a = \ln C_2 + o \ln V_c + p \ln f_z + q \ln a_r + r \ln a_x + \ln \epsilon_2 \tag{5}$$

The linear model of Equation 5 and Equation 6 are described as Equation 6 below:

$$y = \beta_0 + \beta_1 x_1 + \beta_2 x_2 + \beta_3 x_3 + \beta_4 x_4 \tag{6}$$

where y is the R_a or F_c response on a logarithmic scale, x_1 to x_4 is the logarithmic transformation of independent variables, and β_0 to β_4 are the regression coefficients to be estimated. Equation 6 can be rewritten as Equation 7:

$$\hat{y} = y - \epsilon = b_0 + b_1 x_1 + b_2 x_2 + b_3 x_3 + b_4 x_4 \tag{7}$$

where, \hat{y}_i is the determined response, ϵ is the experiment error, b_1 to b_4 are the estimated value of β_0 to β_4 . The quadratic model \hat{y}_2 can be extended as Equation 8:

$$y = y - \epsilon = b_0 + b_1 x_1 + b_2 x_2 + b_3 x_3 + b_4 x_4 + b_{12} x_1 x_2 + b_{13} x_1 x_3 + b_{14} x_1 x_4 + b_{23} x_2 x_3 + b_{24} x_2 x_4 + b_{34} x_3 x_4 + b_{11} x_1^2 + b_{22} x_2^2 + b_{33} x_3^2 + b_{44} x_4^2 \tag{8}$$

To determine the linear quadratic and relationship component of the response using an analysis of variance (ANOVA) method.

2.6 Artificial Neural Networks (ANN)

An ANN is a model for predicting response parameters (dependent variable) using the same principles as biological neural systems. It's one of the most proper analyses in artificial intelligence (AI). ANN can be effectively used to determine the input-output relationship of a complicated process and is considered as a tool in nonlinear statistical data modeling. The ANN structure is built with several neurons on the input layer, hidden layer, and output layer.

The information has processed the neuron and is propagated to other neurons through the synaptic weight of the links connecting the neuron (w_{ij}). Summation the weight input to neurons and including bias is given in Equation 9 [20], [19].

$$y = f \left(\sum_{i=0}^n w_i x_i + \theta \right) \tag{9}$$

where, x_i is the input data, and θ is the bias of the hidden layer. The weighted output is passed-through-

activation-function. The activation functions are used in the hidden and output layer to choose the best activation function that gives the minimum error at output layers during training and testing data. The activation functions are using tansig, logsig, or purelin.

The optimal network configuration during training and testing are found through the calculation of statistical error and commonly are used a function such as Mean Square Error (MSE) and Mean Absolute Percentage Error (MAPE), etc. The error functions are defined by Equation 10 and Equation 11.

$$MSE = \left(\frac{1}{N} \sum_{N=1}^N (t_i - o_i)^2 \right) \tag{10}$$

$$MAPE = \left(\frac{1}{N} \sum_{N=1}^N \left| \frac{t_i - o_i}{o_i} \right| \right) \tag{11}$$

where t is the target value, o is the output value, and N is the number of experiments.

3.0 RESULTS AND DISCUSSION

Surface roughness and cutting force (F_c) results are shown in Table 4. The prediction model using RSM by utilizing the Design Expert 10.0 and ANN by Matlab 14a software.

Table 4 Independent variable and experiment results

Std. Order	Type	Levels of input factor (coded)				Cutting Force F_c (N)	Surface Roughness R_a (μm)
		V_c	f_z	a_r	a_x		
1	Factorial	-1	-1	-1	-1	20.689	0.223
2		1	-1	-1	-1	13.983	0.187
3		-1	1	-1	-1	20.614	0.283
4		1	1	-1	-1	25.616	0.183
5		-1	-1	1	-1	25.085	0.190
6		1	-1	1	-1	22.916	0.176
7		-1	1	1	-1	36.112	0.255
8		1	1	1	-1	39.173	0.270
9		-1	-1	-1	1	29.798	0.187
10		1	-1	-1	1	31.244	0.190
11		-1	1	-1	1	46.511	0.297
12		1	1	-1	1	51.180	0.260
13		-1	-1	1	1	48.152	0.220
14		1	-1	1	1	41.959	0.220
15	-1	1	1	1	61.658	0.238	
16	1	1	1	1	71.003	0.307	
17	Axial	-2	0	0	0	34.918	0.282
18		2	0	0	0	34.050	0.223
19		0	-2	0	0	20.478	0.120
20		0	2	0	0	54.520	0.288
21		0	0	-2	0	24.415	0.195
22		0	0	2	0	53.338	0.275
23		0	0	0	-2	17.439	0.235
24		0	0	0	2	66.817	0.253
25	Center	0	0	0	0	33.707	0.220
26		0	0	0	0	29.288	0.238
27		0	0	0	0	31.062	0.212
28		0	0	0	0	31.204	0.256
29		0	0	0	0	30.240	0.273
30		0	0	0	0	31.762	0.228

The machining force used for analysis is F_c (mean cutting force) that is perpendicular to the thin wall surface. The average arithmetic surface roughness (R_a) is used to measure surface quality, and measurements are made at three times at the end of each workpiece.

3.1 Modelling by RSM

Analysis of variance (ANOVA) is used to analyze the effect of each parameter of Surface roughness and cutting force. The study was set at a significance level as 5% and a confidence level at 95%. Table 5 and Table 6 give the ANOVA result on cutting force and surface roughness of the first order.

Table 5 ANOVA for response surface linear model on cutting force

Source	Sum of Squares	df	Mean Square	F-Value	P-value Prob>F	Remarks
Model	4.51	4	1.13	126.96	< 0.0001	significant
A-Vc	0.0003	1	0.0003	0.0359	0.8512	
B-fz	1.11	1	1.11	125.67	< 0.0001	
C-DOC Rad	0.8890	1	0.8890	100.20	< 0.0001	
D-DOC Ax	2.50	1	2.50	281.93	< 0.0001	
Residual	0.2218	25	0.0089			
Lack of Fit	0.2105	20	0.0105	4.66	0.0477	significant
Pure Error	0.0113	5	0.0023			
Cor Total	4.73	29				

Table 6 ANOVA for response surface linear model on surface roughness

Source	Sum of Squares	df	Mean Square	F-Value	P-value Prob>F	Remarks
Model	0.7351	4	0.1838	10.65	< 0.0001	significant
A-Vc	0.0387	1	0.0387	2.24	0.1468	
B-fz	0.6266	1	0.6266	36.32	< 0.0001	
C-DOC Rad	0.0421	1	0.0421	2.44	0.1307	
D-DOC Ax	0.0278	1	0.0278	1.61	0.2163	
Residual	0.4313	25	0.0173			
Lack of Fit	0.3858	20	0.0193	2.12	0.2066	not significant
Pure Error	0.0454	5	0.0091			
Cor Total	1.17	29				

The first order model in term of coded factors, as follows in Equation 12 and Equation 13:

$$\ln F_c = 3.5 - 0.0036x_1 + 0.2155x_2 + 0.1925x_3 + 0.3228x_4 \tag{12}$$

$$\ln R_a = -1.44 - 0.0401x_1 + 0.1616x_2 + 0.0419x_3 + 0.034x_4 \tag{13}$$

Table 10 Optimum machining parameters for surface roughness

Num ber	V _c	f _z	DOC Rad	DOC Ax	R _a	Desirability
1	125.00	0.040	0.25	5.00	0.161	0.781 Selected
2	124.99	0.040	0.25	5.03	0.161	0.779
3	124.99	0.040	0.25	5.00	0.161	0.779
...

3.2 Modelling by ANN

In this research, ANN analysis using Feedforward Back Propagation (BP). The ANN model optimization is based on (a) the best training algorithm criteria and (b) the number of neurons in the hidden layer. Before train and testing networks, the normalization of input and target data is in the range of -1 and +1, with Equation 18.

$$x_i = \frac{2}{(d_{max} - d_{min})} (d_i - d_{min}) - 1 \quad (18)$$

where, d_{max} and d_{min} are the maximum and minimum values of the row data respectively, while d_i is the input and output data set.

The best training algorithm criteria are determined based on the type of BP algorithm in the matlab toolbox. Training runs on the default parameters value, and some inputs were specified as follows: 10 neurons in the hidden layer, type of learning were learnngd, tansig in hidden and output layer as activation function, the epoch was 1000 and performance goal was MSE/MAPE.

Data for training was selected data-1 to data-28 (87.5%) in Table 4 and testing using data-29, data-30, and data in Table 11 (12.5%).

Table 11 Data for testing

No.	Independent Variables				Cutting Force F _c (N)	Surface Roughness R _a (µm)
	V _c m/min	f _z mm/th	a _r mm	a _x mm		
1	100	0.025	0.4	10	69.26	0.210
2	100	0.063	0.4	10	57.66	0.231

The results of training and testing on different BP algorithms that produce the best MSE/MAPE values for both F_c and R_a are Levenberg-Marquardt, such as shown in Table 11 and Table 12. Therefore, this algorithm was considered as training and testing.

Table 11 The result of training and testing for cutting force

BP Algorithm		MSE	MAPE	R ²
Scaled conjugate gradient	a	0.355	0.5961	0.9992
	b	203.618	17.3214	0.9016
Resilient	a	0.463	1.0515	0.9990
	b	170.973	15.4157	0.9994
Random Weight/Bias Rule	a	2.610	4.3523	0.9943
	b	184.544	16.6667	0.9988
Levenberg-Marquardt	a	1.678	2.7984	0.9962
	b	11.428	5.3469	0.9926
One-step secant	a	2.014	3.6307	0.9955
	b	159.848	15.9503	0.9986
Grad. descent with momentum and adapt. learning rate	a	2.045	3.6969	0.9955
	b	35.227	8.9013	0.9953
gradient descent	a	6.477	6.9838	0.9855
	b	274.566	17.6718	0.7096
Gradient descent with adapting. learning rate	a	5.758	5.3274	0.9870
	b	138.283	13.6154	0.9578
Gradient descent	a	75.515	16.6541	0.8134
	b	166.656	14.6502	0.9484
Conjugate grad. with Polak-Ribière updates	a	0.392	1.0125	0.9991
	b	301.184	20.1655	0.9981
Conjugate grad. with Fletc.-Reeves updates	a	1.136	2.2566	0.9975
	b	177.759	16.9857	0.9922
Conjugate grad. with Powell-Beale restarts	a	0.431	1.2819	0.9990
	b	106.568	9.3596	0.8819
Bayesian regularization	a	7.734	6.8469	0.9831
	b	172.866	13.2503	0.8120
BFGS quasi-Newton	a	0.354	0.5651	0.9992
	b	134.421	14.2471	0.9153

a= Training and b = Testing

Table 12 The result of training and testing for surface roughness

BP Algorithm		MSE	MAPE	R ²
Scaled conjugate gradient	a	0.0000609	2.0812	0.9834
	b	0.0013506	14.1182	0.7226
Resilient	a	0.0000661	2.0962	0.9821
	b	0.0005122	6.4321	0.7036
Random Weight/Bias Rule	a	0.0007217	8.4768	0.8234
	b	0.0008084	11.5665	0.6962
Levenberg-Marquardt	a	0.0000413	0.9546	0.9888
	b	0.0004729	6.1752	0.9540
One-step secant	a	0.0000817	1.9537	0.9777
	b	0.0003162	5.4309	0.7232
Grad. descent with momentum and adapt. learning rate	a	0.0001728	4.0410	0.9522
	b	0.0004718	8.0641	0.7086
gradient descent	a	0.0005176	8.3846	0.8518
	b	0.0008365	11.3186	0.7177
Gradient descent with adapting. learning rate	a	0.0002130	4.9519	0.9416
	b	0.0005819	9.1811	0.7204
Gradient descent	a	0.0008101	10.2770	0.7502
	b	0.0005217	8.7780	0.7210
Conjugate grad. with Polak-Ribière updates	a	0.0000811	2.0652	0.9779
	b	0.0003176	5.3768	0.7263
Conjugate grad. with Fletc.-Reeves updates	a	0.0000667	2.0333	0.9818
	b	0.0004213	5.2342	0.7225
Conjugate grad. with Powell-Beale restarts	a	0.0002056	5.0740	0.9431
	b	0.0011474	13.3064	0.7230
Bayesian regularization	a	0.0000806	2.8561	0.9805
	b	0.0004590	4.6738	0.5773
BFGS quasi-Newton	a	0.0000413	0.9547	0.9888
	b	0.0024770	15.8320	0.6591

a= Training and b = Testing

The optimum number of neurons in the hidden layer is determined based on the MSE/MAPE after training and testing. There is no standard rule about the number of hidden layers, and it depends on the specifications and complexity of the experimental data. Many researchers only use a hidden layer to obtain optimal conditions [22], [23], [19].

The ANN structure chosen in this study was 4-n-1, where n is the number of neurons in the hidden layer, as shown in Figure 2. The results of training to obtain the best network performance for the number of neurons 1 to 20 are shown in Figure 3 and Figure 4.

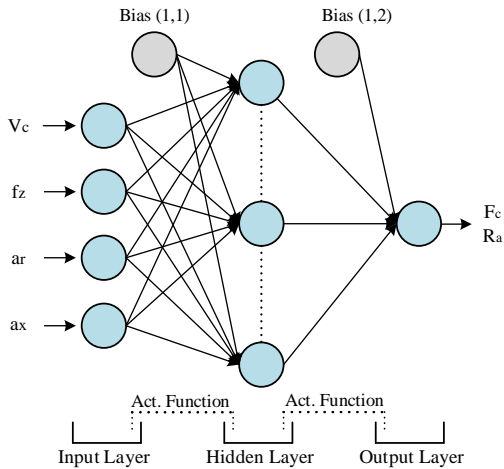


Figure 2 ANN with architecture 4-n-1 (n is the sum of neuron in the hidden layer)

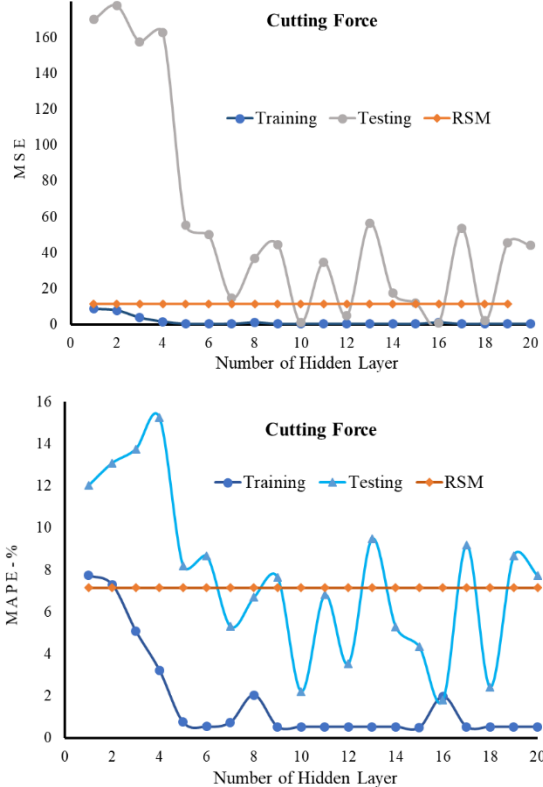


Figure 3 The network's performance in the hidden layer for cutting force

Experimental results and prediction with RSM and ANN are presented in Table 13 and Table 14. It was observed that the range of error percentage RSM is -15.09 to 18.307 % at F_c and -35.62 to 22.84 % at R_a . Error percentage between experiment result and ANN is -6.922 to 7.096 % at F_c and -9.198 to 15.202 % at R_a . From the prediction results between these two models, the percentage error ANN models are significantly better than the RSM model. The developed ANN model can be effectively utilized for prediction of F_c and R_a .

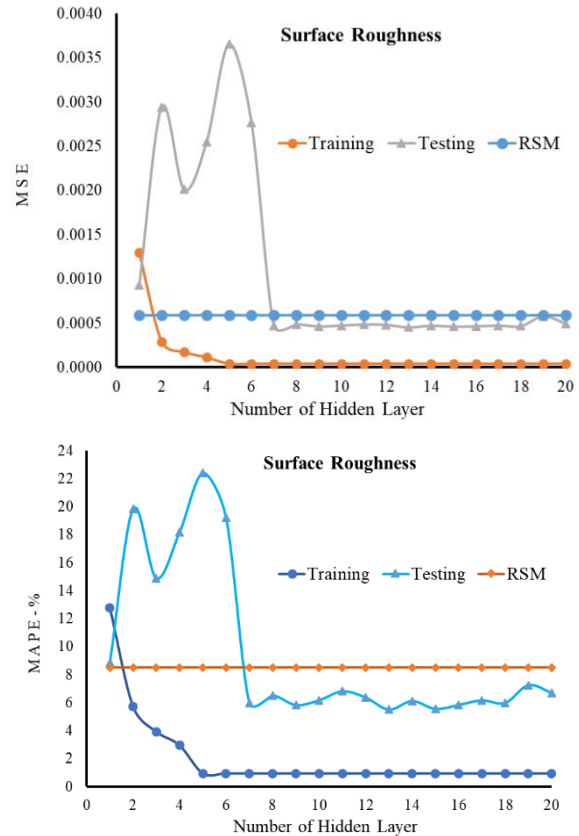


Figure 4 The network's performance in the hidden layer for surface roughness

Table 13 The value of experiment and prediction F_c

N	Average F_c Exp. (N)	RSM		ANN	
		Predicted	% Error	Predicted	% Error
1	20.689	17.936	13.30	20.689	0.000004
2	13.983	14.805	-5.88	13.984	-0.008784
3	20.614	23.024	-11.69	20.614	-0.000001
4	25.616	25.069	2.14	25.616	-0.000040
5	25.085	26.786	-6.78	25.085	0.000003
6	22.916	22.253	2.89	22.916	0.000000
7	36.112	35.548	1.56	36.112	0.000000
8	39.173	38.956	0.55	39.173	0.000000
9	29.798	33.151	-11.25	29.798	0.000001
10	31.244	29.719	4.88	31.244	0.000011
11	46.511	44.846	3.58	46.511	0.000000
12	51.180	53.033	-3.62	51.18	0.000000
13	48.152	46.068	4.33	48.152	0.000002
14	41.959	41.566	0.94	41.959	0.000000
15	61.658	64.430	-4.50	61.658	-0.000001
16	71.003	76.686	-8.00	71.002	0.000898
17	34.918	30.326	13.15	34.918	0.000002

N	Average	RSM		ANN	
		o	F _c Exp. (N)	Predicted	% Error
18	34.050	29.064	14.64	34.05	-0.000002
19	20.478	21.837	-6.64	20.478	0.000000
20	54.520	58.332	-6.99	54.52	-0.000003
21	24.415	22.200	9.07	24.415	0.000000
22	53.338	53.906	-1.06	53.338	-0.000001
23	17.439	18.307	-4.98	17.439	0.000000
24	66.817	76.901	-15.09	66.817	0.000001
25	33.707	27.562	18.23	31.315	7.095716
26	29.288	27.562	5.89	31.315	-6.921767
27	31.062	27.562	11.27	31.315	-0.815296
28	31.204	27.562	11.67	31.315	-0.356516
29	30.240	27.562	8.85	31.315	-3.555711
30	31.762	27.562	13.22	31.315	1.406564

Table 14 The value of experiment and prediction R_a

N	Average	RSM		ANN	
		o	R _a Exp. (N)	Predicted	% Error
1	0.223	0.214	3.85	0.223	-0.000001
2	0.187	0.160	14.69	0.187	-0.000003
3	0.283	0.283	0.06	0.283	0.000000
4	0.183	0.209	-14.40	0.183	0.000000
5	0.190	0.198	-4.37	0.190	0.000001
6	0.176	0.188	-6.68	0.176	0.000001
7	0.255	0.271	-6.27	0.255	0.000003
8	0.270	0.255	5.46	0.270	0.000003
9	0.187	0.197	-5.53	0.187	-0.000003
10	0.190	0.178	6.36	0.190	-0.000001
11	0.297	0.277	6.72	0.297	0.000000
12	0.260	0.248	4.43	0.260	0.000000
13	0.220	0.191	13.01	0.220	0.000005
14	0.220	0.220	0.19	0.220	0.000011
15	0.238	0.278	-16.94	0.238	0.000000
16	0.307	0.318	-3.49	0.307	0.001234
17	0.282	0.258	8.40	0.282	0.000001
18	0.223	0.214	4.17	0.223	0.000001
19	0.120	0.163	-35.62	0.120	-0.003927
20	0.288	0.222	22.84	0.288	0.000002
21	0.195	0.212	-8.87	0.195	-0.000002
22	0.275	0.237	13.70	0.275	0.000003
23	0.235	0.223	5.03	0.235	0.000000
24	0.253	0.255	-0.81	0.253	0.000001
25	0.220	0.227	-3.03	0.231	-5.227273
26	0.238	0.227	4.76	0.231	2.731093
27	0.212	0.227	-6.92	0.231	-9.198113
28	0.256	0.227	11.46	0.231	9.570313
29	0.273	0.227	16.97	0.231	15.20147
30	0.228	0.227	0.58	0.231	-1.535088

3.3 The Effect of Independent Variables Toward Dependent Variables

Figure 5 shows the perturbation plot between Independent and dependent variables for cutting force and surface roughness. It was clear that with the increase of feed (B), DOC radial (C) and DOC axial (C), dependent variables increased due to an increase in the cross-sectional area of the chip. The opposite phenomenon, an increase of cutting speed (A) resulted in a decrease of dependent variables (F_c and R_a). Usually, the cutting temperature increases with increasing cutting speed and causes a decrease in hardness in the tool contact area of the workpiece,

thereby reducing cutting energy. This effect causes a reduction in the cutting force and surface of the workpiece to be smooth [24]. The impact of B, C, D on cutting force was more significant than surface roughness.

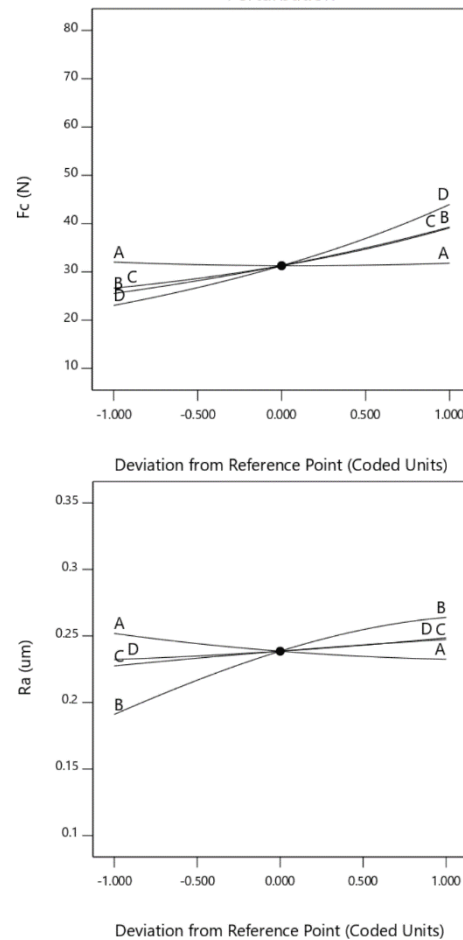


Figure 5 Perturbations plot for cutting force and surface roughness

4.0 CONCLUSION

The application of the RSM and the ANN for optimum performance on end milling thin walled Ti6Al4V has been presented in this paper. The result of the analysis has shown that the second order RSM models and Levenberg-Marquardt algorithm in the ANN network were developed to predict the F_c and R_a values from experimental data. The prediction data by RSM and ANN are very close to the data obtained from the experimental results. The training and testing results of network structure 4-10-1 for F_c and 4-13-1 for R_a shows better accuracy than RSM predictions.

From the development of the model shows that the f_z cause the most significant effect on F_c and R_a, followed by a_x and a_r. And contrary to the influence of the V_c where the increase of the V_c reduced F_c and R_a. The optimum condition was determined based on the minimum value of F_c and R_a on the independent

variable range. Optimum condition at $V_c = 125$ m/min, $f_z = 0.04$ mm/tooth, $a_r = 0.25$ mm and $a_d = 5$ mm which resulted F_c and R_a were 14.89 N and $0.161 \mu\text{m}$, respectively.

Acknowledgment

The authors wish to thank Sriwijaya University (Unsri) and Universiti Teknologi Malaysia (UTM) for the cooperation and assistance under the research collaboration between both universities. Special appreciation to the Research Management Centre of UTM for the financial support through the RUG funding Q.J130000.2409.04G39.

References

- [1] Bolar, G., Das, A., and Joshi, S. N. 2018. Analysis of Surface Integrity and Dimensional Accuracy During Thin-Wall Machining BT - Techno-Societal 2016. In: Pawar, P. M., Ronge, B. P., Balasubramaniam, R., Seshabhatar, S., editors. *Proceedings of the International Conference on Advanced Technologies for Societal Applications, Techno-Societal 2016*. Cham: Springer International Publishing. 681-8.
- [2] Huang, P. L., Li, J. F., Sun, J., and Jia, X. M. 2016. Cutting Signals Analysis in Milling Titanium Alloy Thin-part Components and Non-thin-wall Components. *International Journal of Advanced Manufacturing Technology* 84(9): 2461-9. Doi: 10.1007/s00170-015-7837-0.
- [3] Feng, J., Sun, Z., Jiang, Z., and Yang, L. 2016. Identification of Chatter in Milling of Ti-6Al-4V Titanium Alloy Thin-walled Workpieces based on Cutting Force Signals and Surface Topography. *International Journal of Advanced Manufacturing Technology* 82(9-12): 1909-20. Doi: 10.1007/s00170-015-7509-0.
- [4] Jiang, Z. H., Jia, M. F., and Liu, P. H. 2017. Experimental Study on Milling Force in Processing Ti6Al4V Thin-walled Part 154(Icmia). 486-515.
- [5] Park, K.-H., Suhaimi, M. A., Yang, G.-D., Lee, D.-Y., Lee, S.-W., and Kwon, P. 2017. Milling of Titanium Alloy with Cryogenic Cooling and Minimum Quantity Lubrication (MQL). *International Journal of Precision Engineering and Manufacturing*. 18(1): 5-14. Doi: 10.1007/s12541-017-0001-z.
- [6] Srikanth, R. R. and Rao, P. N. 2017. Use of Vegetable-based Cutting Fluids for Sustainable Machining. Doi: 10.1007/978-3-319-51961-6.
- [7] Huang, Y. A., Zhang, X., and Xiong, Y. 2012. Finite Element Analysis of Machining Thin-Wall Parts: Error Prediction and Stability Analysis. In: Ebrahimi, F., editor. *Finite Element Analysis-Applications in Mechanical Engineering*. 1st ed. In Tech. 327-54.
- [8] Debnath, S., Reddy, M. M., and Yi, Q. S. 2014. Environmental Friendly Cutting Fluids and Cooling Techniques in Machining: A Review. *Journal of Cleaner Production* 83(November): 33-47. Doi: 10.1016/j.jclepro.2014.07.071.
- [9] Boswell, B., Islam, M. N., Davies, I. J., Ginting, Y. R., and Ong, A. K. 2017. A Review Identifying the Effectiveness of Minimum Quantity Lubrication (MQL) During Conventional Machining. *International Journal of Advanced Manufacturing Technology*. Feb.: 1-20. Doi: 10.1007/s00170-017-0142-3.
- [10] Sharif, M. N., Pervaiz, S., and Deiab, I. 2017. Potential of Alternative Lubrication Strategies for Metal Cutting Processes: A Review. *International Journal of Advanced Manufacturing Technology*. Doi: 10.1007/s00170-016-9298-5.
- [11] Sharma, V. S. S., Singh, G., and Sørby, K. 2015. A Review on Minimum Quantity Lubrication for Machining Processes Machining Processes. *Machining Science and Technology* 30(8): 935-53. Doi: 10.1080/10426914.2014.994759.
- [12] Sodavadia, K. P. and Makwana, A. H. 2014. Experimental Investigation on the Performance of Coconut oil Based Nano Fluid as Lubricants during Turning of AISI 304 Austenitic Stainless Steel. *International Journal of Advanced Mechanical Engineering*. 4(1): 55-60.
- [13] Rahim, E. A. and Sasahara, H. 2011. Investigation of Tool Wear and Surface Integrity on MQL Machining of Ti-6AL-4V using Biodegradable Oil. *Proceeding of the Institution of Mechanical Engineers, Part B: Journal of Engineering Manufacture* 225(9): 1505-10. Doi: 10.1177/0954405411402554.
- [14] Armendia, M., Garay, A., Iriarte, L., and Arrazola, P. 2010. Comparison of the Machinabilities of Ti6Al4V and TIMETAL ® 54M using Uncoated WC – Co Tools. *Journal of Materials Processing Technology*. 210: 197-203. Doi: 10.1016/j.jmatprotec.2009.08.026.
- [15] Rahman Rashid, R. A., Palanisamy, S., Sun, S., and Dargusch, M. S. 2016. Tool Wear Mechanisms Involved in Crater Formation on Uncoated Carbide Tool when Machining Ti6Al4V Alloy. *International Journal of Advanced Manufacturing Technology*. 83(9-12): 1457-65. Doi: 10.1007/s00170-015-7668-z.
- [16] Bolar, G. and Joshi, S. N. 2017. Three-dimensional Numerical Modeling, Simulation and Experimental Validation of Milling of a Thin-wall Component. *Proceedings of the Institution of Mechanical Engineers, Part B: Journal of Engineering Manufacture*. 231(5): 792-804. Doi: 10.1177/0954405416685387.
- [17] Rao, R. V. and Kalyankar, V. D. 2014. Optimization of Modern Machining Processes using Advanced Optimization Techniques: A Review. *The International Journal of Advanced Manufacturing Technology*. 1159-88. Doi: 10.1007/s00170-014-5894-4.
- [18] Myers, R. H., Montgomery, D. C., and Anderson-Cook, C. M. 2009. *Response Surface Methodology: Process and Product Optimization Using Designed Experiments*. 3rd ed. Hoboken, New Jersey (USA), United States of America (USA): John Wiley & Sons, Inc.
- [19] Mohrni, A. S., Yanis, M., Sharif, S., Yani, I., Yuliwati, E., Ismail, A.F., et al. 2017. A Comparison RSM and ANN Surface Roughness Models in Thin-wall Machining of Ti6Al4V using Vegetable Oils under MQL-condition. *AIP Conference Proceedings* 1885(020161): 1-10. Doi: 10.1063/1.5002355.
- [20] Kilickap, E., Yardimeden, A., and Çelik, Y. H. 2017. Mathematical Modelling and Optimization of Cutting Force, Tool Wear and Surface Roughness by using Artificial Neural Network and Response Surface Methodology in Milling of Ti-6242S. *Applied Sciences*. 7(10): 1064. Doi: 10.3390/app7101064.
- [21] Sangwan, K. S., Saxena, S., and Kant, G. 2015. Optimization of Machining Parameters to Minimize Surface Roughness using Integrated ANN-GA Approach. *Procedia CIRP* 29: 305-10. Doi: 10.1016/j.procir.2015.02.002.
- [22] Kant, G. and Sangwan, K. S. 2015. Predictive Modelling and Optimization of Machining Parameters to Minimize Surface Roughness using Artificial Neural Network Coupled with Genetic Algorithm. *Procedia CIRP* 31(CIRP 15): 453-8. Doi: 10.1016/j.procir.2015.03.043.
- [23] Sehgal, A. K. 2014. Application of Artificial Neural Network in Surface Roughness Prediction considering Mean Square Error as Performance Measure. 72-6.
- [24] Ozel, T., Thepsonthi, T., Ulutan, D., Kaffanoglu, B. 2011. Experiments and Finite Element Simulations on Micro-Milling of Ti-6Al-4V Alloy with Uncoated and cBN Coated Micro-Tools. *CIRP Ann Manuf Technol*. 60: 85-88. Doi: 10.1016/j.cirp.2011.03.087.